PAPER

Check for updates

CuFe₂O₄-catalyzed one-pot synthesis of α-substituted 2-benzofuranmethamines *via* tandem A³ coupling, 5-*exo*-dig cyclization, and 1,3-allylic rearrangement

Ashok Kumar Raigar, [ID] Manju, [ID] Kamlesh Saini [ID] and Anjali Guleria [ID] *

A one-pot strategy was developed for the synthesis of α-substituted 2-benzofuranmethamines from salicylaldehydes, phenylacetylenes, and cyclic secondary amines using CuFe₂O₄ as a bifunctional catalyst. The reaction proceeds at 80 °C in 1,4-dioxane using Cs₂CO₃ as a base, enabling sequential A³-coupling, 5-*exo*-dig cyclization, and 1,3-allylic rearrangement in a single operation. Unlike previous methods, this protocol employs non-precious metal catalysts and mild reagents, operates under moderate conditions, and provides direct access to α-substituted 2-benzofuranmethamines in good yields (80–96%) with broad substrate compatibility. Furthermore, the catalyst is magnetically recoverable and exhibits excellent reusability over five consecutive cycles without significant loss of activity.

Introduction

α-Aryl-2-benzofuranmethamines are of significant interest in medicinal chemistry due to their broad pharmacological profile. Compounds bearing this scaffold (Fig. 1 and 5) have been identified as σ₁ receptor ligands, which are implicated in modulating neuroprotective and neuromodulatory pathways.[1] Additionally, they function as calcium channel antagonists,[3] exhibit analgesic activity,[2] and have been reported to possess therapeutic applications in the management of allergic responses, arrhythmia, and tussive conditions.[4] In one of the early synthetic approaches, Pestellini *et al.*[4] reported the preparation of compounds of generalized structure 5 *via* a stepwise sequence involving functional group interconversions (Fig. 1). The route began with nucleophilic addition of 2-lithiobenzofuran (b) to an aryl aldehyde (a) to afford benzylic alcohols (c), followed by chlorination to give chlorides (d), which were subsequently subjected to nucleophilic substitution with amines. While chemically robust, this approach relies on moisture-sensitive organolithium reagents, halogenating agents, and multistep protocols, factors that limit its scalability and conflict with green chemistry principles. These drawbacks have motivated the development of more concise, convergent, and sustainable strategies.

In subsequent years, McLean *et al.*[5] and Nun *et al.*[6] independently reported the synthesis of a single α-aryl-2-benzofuranmethamine, 4-(2-benzofuranylphenylmethyl)morpholine, *via* the Petasis boronic acid Mannich reaction under

microwave irradiation, with yields ranging from 23%[5] to 95%.[6] While their studies broadly focused on microwave-assisted Petasis chemistry and produced various 2-hydroxyaryl derivatives, only one compound bearing this scaffold was reported. Nonetheless, the protocols required high temperatures and energy input, and in the case of McLean *et al.*, delivered modest yields (Fig. 2).

A significant advancement was later reported by Wongsa *et al.*,[7] who developed a two-step protocol for synthesizing 5 using salicylaldehyde, phenylacetylene, and cyclic/acyclic secondary amines as starting materials. The method involved an initial AgNO₃-catalyzed 5-*exo*-dig cycloisomerization of the A³-coupling product 4 to afford 2-arylmethylidenebenzofurans (4′), followed by a second step, an AgNO₃-promoted 1,3-allylic rearrangement under Lewis acidic conditions, conducted at 100 °C over 18 hours to deliver the target compound 5 (Fig. 2). While the protocol successfully provided access to the desired
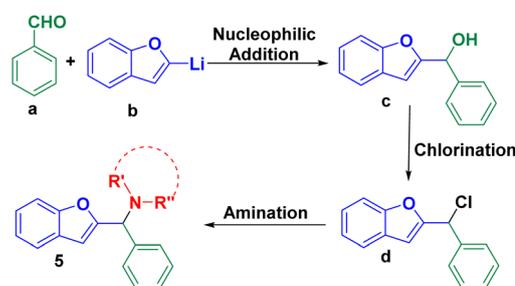

Fig. 1 Multistep synthesis of α-aryl-2-benzofuranmethamines (**5**) *via* carbinol intermediates (**c**) and corresponding chlorides (**d**), as reported by Pestellini *et al.* (*US Pat.* 4485112, 1984).

Department of Chemistry, University of Rajasthan, Jaipur 302004, India. E-mail: dranjaliguleria@uniraj.ac.in
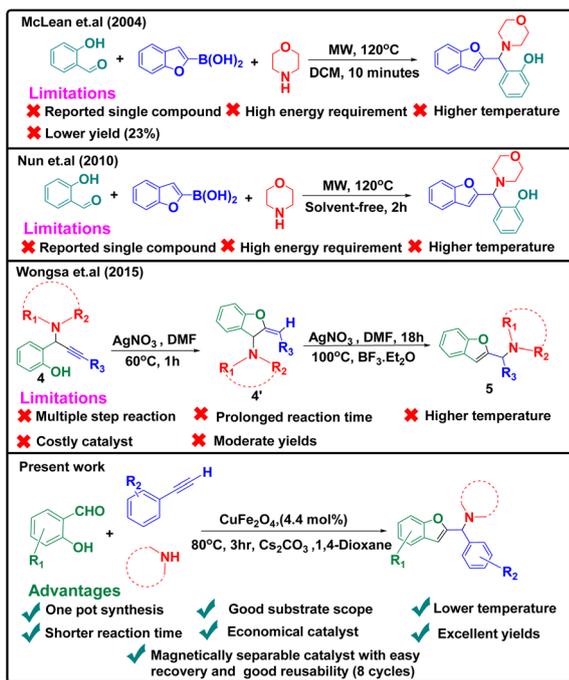
Fig. 2 Comparison of more recent catalytic strategies and the present CuFe$_2$O$_4$-catalyzed one-pot protocol for synthesizing α-substituted 2-benzofuranmethamines.

scaffold in moderate to good yields, it was limited by its multistep nature, high temperature, extended reaction times, formation of by-products, and reliance on a costly silver-based catalyst.

Encouraged by the findings of Wongsa et al.,[7] we sought to develop a more sustainable catalytic system that addresses the key operational and environmental limitations of previous methods. Our attention turned to several parallel studies that described the synthesis of either 2-aryl(alkyl)methylidenebenzofurans (4′) or 2-aryl(alkyl)-3-aminobenzofurans (6) through copper-catalyzed processes (Fig. 3).

Ukhin et al.[8] reported the synthesis of 4′ from the propargylamine intermediate A, prepared via condensation of salicylaldehyde with secondary amines and propargyl alcohols.
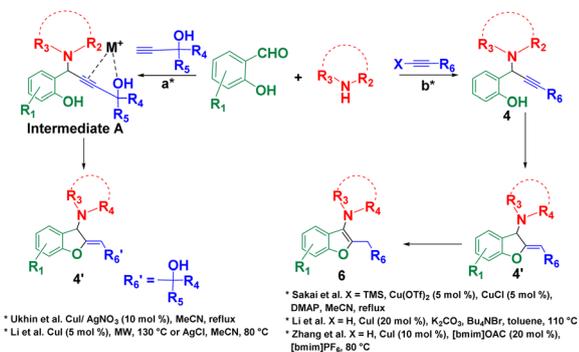

Fig. 3 Previous studies demonstrating the role of copper catalysis in the synthesis of benzofuran derivatives (4′ and 6) through tandem cyclization and isomerization pathways.

Further cyclization using either AgNO$_3$ or CuI (10 mol%) in MeCN under reflux (15–40 min) gave products 4′ in 39–74% yield. These findings were supported by Nguyen et al.,[9] who demonstrated that microwave-assisted treatment of salicylaldehyde with cyclic amines and propargyl alcohols or alkynes bearing remote hydroxyl groups, in the presence of CuI (5 mol%) at 130 °C for 30 min, afforded 4′ in 44–88% yield. Conditions employing AgCl (5 mol%) in MeCN at 80 °C for 16 h were also effective, though they gave slightly lower yields. Interestingly, 3,3-dimethylbut-1-yne failed to cyclize, suggesting that the hydroxyl group in the alkyne plays a key role in metal-assisted coordination during the cyclization (intermediate A).

Sakai et al.[10] advanced the method by eliminating the need for a propargylic hydroxyl group. They employed salicylaldehyde (1.5 equiv.), a secondary amine (1 equiv.), and 1-TMS-alkynes (1.5 equiv.), with Cu(OTf)$_2$ (5 mol%), CuCl (5 mol%), and DMAP (1 equiv.) in MeCN at reflux for 6 h. Their results indicated that 4′, though not isolated, underwent base-induced isomerization to 6 in variable yields (22–99%). Later, a related study by Li et al.[11] further supported this transformation using salicylaldehyde (2 equiv.), a secondary amine (1 equiv.), and a terminal alkyne (1.5 equiv.) in the presence of CuI (20 mol%), K$_2$CO$_3$ (1 equiv.), and Bu$_4$NBr (1 equiv.) in toluene at 110 °C for 2–3 h. Notably, in the absence of a base, the propargylamine intermediate 4 was isolated in 84% yield. Moreover, use of 1-octyne gave a separable mixture of 4′ and 6 (~1 : 1), suggesting that under less basic or milder conditions, compounds with the general structure 4′ may be stabilized or isolated more selectively. These findings influenced our decision to conduct the reaction under basic conditions to suppress the formation of 4′ as the predominant product.

Zhang et al.[12] later reported that related cyclizations to afford 6 could be performed using salicylaldehyde, a secondary amine (1.2 equiv.), and a terminal alkyne (1.5 equiv.) with CuI (10 mol%) and [bmim]OAc (20 mol%) in [bmim]PF$_6$ at 80 °C for 6–9 h. Additionally, several other cyclization reactions of propargyl alcohol analogues of 4 (R^6=H or aryl) were reported by Harkat et al. and several other research groups[13] to yield 3-hydroxy-2,3-dihydro-2-arylmethylidenebenzofurans (analogues of 4′), which could undergo rearrangement to 2-hydroxymethylbenzofurans or 2-alkoxybenzofurans under acidic or alcoholic conditions.

Together, these studies highlighted the versatility of copper-based systems in promoting both cyclization and rearrangement processes relevant to our scaffold. Thus, building on these mechanistic insights and the established role of Lewis acids in promoting 1,3-allylic rearrangements, we hypothesized that CuFe$_2$O$_4$, a mixed-metal oxide containing both Cu^{2+} and Fe^{3+} centers, could serve as an effective dual-function catalyst.[14] These metal centers are known to exhibit Lewis acidity, which could promote not only the initial A^3-coupling and cyclization but also the subsequent 1,3-allylic rearrangement. Furthermore, CuFe$_2$O$_4$ offers practical advantages such as low cost, magnetic recoverability, excellent reusability for up to five cycles without significant loss of activity, and overall environmental compatibility. The operational and environmental advantages

of our protocol compared to previous strategies are illustrated in Fig. 2

As a Brønsted base, Cs_2CO_3 was selected due to its reliable solubility in polar aprotic solvents and its common use in multicomponent and rearrangement reactions. Its use allowed us to avoid strongly basic or nucleophilic additives that might interfere with Lewis acidic centers or promote undesired side reactions. Finally, 1,4-dioxane was chosen as the reaction solvent owing to its high boiling point, chemical stability, and ability to solubilize both organic and inorganic components, enabling efficient progression of the reaction under mild thermal conditions.

Thus, we developed a one-pot transformation that integrates the key steps of A³-coupling, cycloisomerization, and 1,3-allylic rearrangement within a single catalytic system. $CuFe_2O_4$ was employed as a bifunctional catalyst, with surface Cu^{2+} and Fe^{3+} centers capable of activating alkynes, stabilizing intermediates, and promoting the Lewis acid-driven 1,3-allylic rearrangement. Cs_2CO_3 was chosen as a mild, soluble base compatible with the catalytic system, and the reaction was performed in 1,4-dioxane, a thermally robust and chemically suitable solvent. This approach addresses the synthetic and environmental limitations of previous methods by streamlining the process, minimizing manipulations, and eliminating the need for precious metal catalysts, harsh reagents, and elevated temperatures. In addition to operational simplicity, the protocol delivers good yields across a broad substrate scope and employs a magnetically separable catalyst that retains high activity over five consecutive cycles without significant loss of efficiency. Hence,

the work presented herein demonstrates the utility of this strategy, delineates its scope, and evaluates its potential as a more sustainable and broadly applicable method for the synthesis of α-substituted 2-benzofuranmethamines.

Result and discussion

Optimization studies for the synthesis of $CuFe_2O_4$ catalyzed 1-(benzofuran-2-yl(phenyl)methyl)-3-methylpiperidine (5a)

To identify the optimal conditions for the synthesis of 1-(benzofuran-2-yl(phenyl)methyl)-3-methylpiperidine (5a), the reaction between phenylacetylene (1a), 3-methylpiperidine (2a), and salicylaldehyde (3a) was selected as a model and systematically evaluated for catalyst loading, solvent effects, temperature, and reaction time (Table 1).

In the absence of both catalyst and solvent, no reaction occurred, even after prolonged heating at room temperature (RT) or reflux (entry 1). Similarly, conducting the reaction in water, ethanol, or their mixtures (1 : 1 v/v, reflux temperature = 78.15 °C) without a catalyst resulted in no product formation (entry 2), indicating that neither polar protic media nor thermal activation alone were sufficient to promote the transformation.

When 2 mol% $CuFe_2O_4$ was introduced under the same solvent systems (water, ethanol, or $EtOH/H_2O$ mixtures), only trace product formation was observed after 180 minutes, regardless of temperature (entry 3). This demonstrated that these protic environments are unsuitable for catalysis, likely due to poor solubility or deactivation of the catalytic surface.

Table 1 Optimization studies for the synthesis of 1-(benzofuran-2-yl(phenyl)methyl)-3-methylpiperidine (5a)[a]
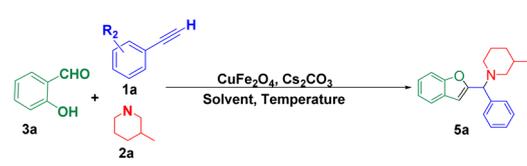
Entry	Catalyst (%)	Solvent	Temp. (°C)	Time (min)	Yield[b] %
1	—	—	RT, reflux	600	No reaction
2	—	H_2O, EtOH, H_2O/EtOH(1 : 1)	RT, reflux	600	No reaction
3	2	H_2O, EtOH, H_2O/EtOH(1 : 1)	RT, reflux	180	Traces
4	2	Toluene	RT, reflux	180	Traces, 22[c]
5	2	DMSO	RT, reflux	180	Traces, 26[c]
6	2	1,4-Dioxane	RT	180	12[c]
7	2	1,4-Dioxane	50, 70	180	42[c], 51[c]
8	4.4	1,4-Dioxane	RT, 50	180	36[c], 66[c]
9	4.4	1,4-Dioxane	80	60	68[c]
10	4.4	1,4-Dioxane	80	120	78[c]
11	**4.4**	**1,4-Dioxane**	**80**	**180**	**97, 94[d]**
12	4.4	1,4-Dioxane	Reflux	180	97
13	4.4	1,4-Dioxane	80	240	97
14	8.8	1,4-Dioxane	80	180	97
15	15	1,4-Dioxane	80	180	97

[a] Reaction conditions: salicylaldehyde (1.0 mmol, 0.12 mL), phenylacetylene (1.1 mmol, 0.14 mL), 3-methylpiperidine (1.3 mmol, 0.12 mL), cesium carbonate (0.31 mmol, 0.10 g), 1,4-dioxane (5 mL), and the required amount of the catalyst were treated at the indicated temperatures. [b] Isolated yields after column chromatography. [c] Reactions did not reach completion within the indicated times, and extended durations up to 600 minutes yielded no further conversion, as confirmed by TLC using ethyl acetate/hexane (2 : 8) as eluent. [d] Under N_2 using dry 1,4-dioxane as solvent.

The solvent effect was further examined using organic media. In toluene and DMSO, only trace formation was observed at RT; however, upon heating to reflux, yields improved modestly to 22% and 26%, respectively (entries 4 and 5). These results suggested that while nonpolar (toluene) and polar aprotic (DMSO) solvents could partially enable the reaction under forcing conditions, the conversion remained incomplete, likely due to limited solubility of the base or suboptimal stabilization of reactive intermediates.

1,4-Dioxane proved superior in promoting the reaction. At RT with 2 mol% catalyst, a 12% yield was observed (entry 6), which increased significantly to 42% at 50 °C and 51% at 70 °C under identical conditions (entry 7). This established both solvent identity and temperature as key variables. Increasing the catalyst loading to 4.4 mol% further improved the performance, affording 36% yield at RT and 66% at 50 °C (entry 8).

To refine the protocol further, the reaction was examined at 80 °C. At this temperature and 4.4 mol% catalyst loading, a 68% yield was obtained after 60 minutes (entry 9), increasing to 78% at 120 minutes (entry 10), and reaching full conversion (97%) at 180 minutes (entry 11). Interestingly, conducting the same reaction under an inert nitrogen atmosphere using dried 1,4-dioxane gave a slightly lower yield of 94%, suggesting that ambient conditions may subtly influence catalyst surface activity or solvation effects (entry 11, footnote d).

Neither prolonging the reaction time to 240 minutes nor raising the temperature to reflux further improved the yield, which remained at 97% (entries 12 and 13). These observations confirmed that 80 °C for 180 minutes is the most efficient condition. Increasing the catalyst loading to 8.8 and 15 mol% (entries 14 and 15) also showed no additional benefit, demonstrating that 4.4 mol% $CuFe_2O_4$ is sufficient to achieve maximum conversion.

A control reaction performed under the optimized conditions in the absence of Cs_2CO_3 revealed that the primary product was the A^3-coupling intermediate, 1-(phenyl(2-hydroxybenzyl))-3-methylpiperidine (**4a**), with negligible formation of the target product. This finding highlights the crucial role of the base in enabling the 5-*exo*-dig cyclization that leads to subsequent 1,3-allylic rearrangement.

In conclusion, the optimized conditions for this transformation were established as 4.4 mol% $CuFe_2O_4$ and 0.31 mmol Cs_2CO_3 in 1,4-dioxane at 80 °C for 180 minutes, affording the desired product **5a** in excellent isolated yield (97%).

$CuFe_2O_4$ catalyzed synthesis and substrate scope of α-aryl-2-benzofuranmethamines derivatives (5a–h)

With the optimized conditions established, the reaction scope was evaluated using representative salicylaldehydes, terminal aryl alkynes, and cyclic secondary amines (Scheme 1). The transformation delivered α-aryl-2-benzofuranmethamines (**5a–h**) in good to excellent yields (80–96%) across all combinations. Substituents on the salicylaldehyde, aryl alkyne, and amine rings, including electron-donating and electron-withdrawing groups, had minimal influence on the reaction outcome,
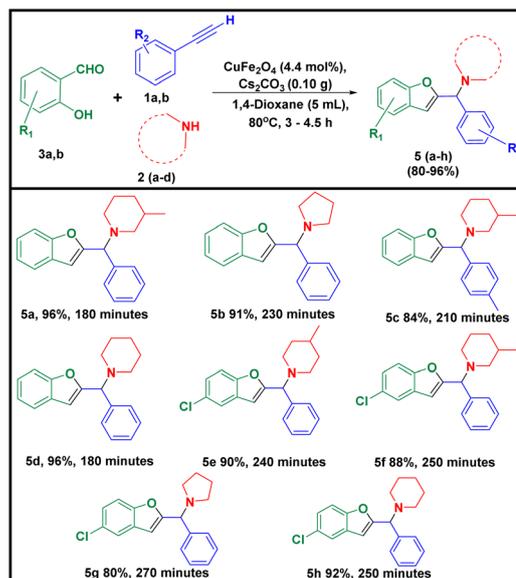

Scheme 1 Synthesis and substrate scope of α-aryl-2-benzofuranmethamines derivatives (**5a–h**).

reflecting the method's tolerance to varied electronic environments. A modest decrease in yield was observed with pyrrolidine derivatives, likely due to increased ring strain and reduced conformational flexibility compared to six-membered amines, which may influence the efficiency of cyclization and rearrangement. Overall, the protocol proved reliable across structurally and electronically diverse inputs.

Mechanism

A plausible mechanism for the $CuFe_2O_4$-catalyzed synthesis of α-aryl-2-benzofuranmethamines (**5a–h**) is illustrated in Scheme 2. The reaction likely begins with a $CuFe_2O_4$- and base-assisted
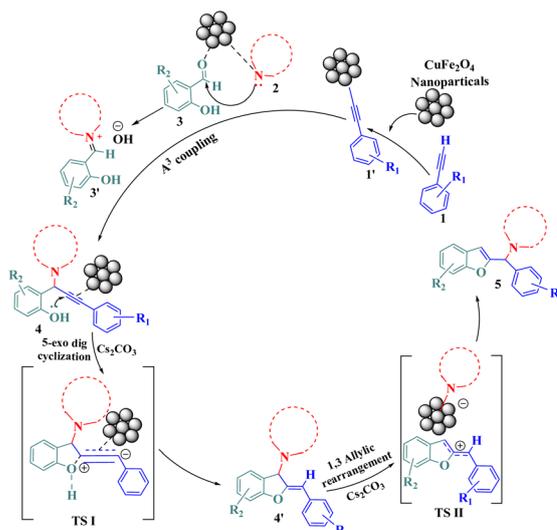
Scheme 2 A plausible mechanism for the $CuFe_2O_4$ nanoparticles catalyzed synthesis of α-aryl-2-benzofuranmethamines (**5a–h**).

A^3 coupling between salicylaldehyde (**3**), a terminal aryl alkyne (**1**), and a cyclic secondary amine (**2**). Under basic conditions, Cs_2CO_3 deprotonates the terminal alkyne to generate an acetylide species (**1'**), which adds to an iminium intermediate (**3'**) formed *in situ via* $CuFe_2O_4$-facilitated activation of both the carbonyl and amine functionalities. The resulting propargylamine intermediate (**4**) is then formed through this multicomponent coupling.

The resulting intermediate (**4**) then undergoes a 5-*exo*-dig cyclization, aided by Cs_2CO_3-mediated deprotonation of the phenolic hydroxyl. At the same time, $CuFe_2O_4$ may assist the process through a metal coordination interaction with the alkyne, helping to align the reacting centers for smooth ring closure.

This gives rise to intermediate (**4'**), presumed to be a benzofuranylmethylidene species, which subsequently undergoes a 1,3-allylic rearrangement to yield the final product (**5**). As expected in a one-pot protocol, intermediate **4'** was not isolated, which aligns with previous reports where similar species were formed transiently and not separated.[10–12] In this rearrangement step, $CuFe_2O_4$ might act as a Lewis acid, owing to its Cu^{2+} and Fe^{3+} surface sites, facilitating conversion to the final product through transition state II. The basic environment provided by Cs_2CO_3 likely plays a supporting role in enabling charge reorganization. Altogether, this process integrates multicomponent coupling, cyclization, and rearrangement into a single operational sequence under mild conditions using a recyclable and magnetically recoverable catalyst.

Reusability and recovery of the catalyst

To evaluate the reusability and stability of $CuFe_2O_4$, the model reaction corresponding to Table 1, entry 11, was selected for the synthesis of compound **5a**. After each cycle, the catalyst was separated from the reaction mixture with an external magnet, washed thoroughly with petroleum ether, and dried at 60 °C for three hours before being reused. This procedure was repeated for five consecutive cycles.

The catalyst consistently delivered high yields with minimal change in reaction time across all cycles, indicating excellent retention of catalytic activity (Fig. 4). After the fifth run, 9.2 mg of catalyst was recovered from the initial 10 mg, corresponding to 92% mass recovery. The modest loss (∼8%) is likely

attributable to mechanical handling during separation and washing rather than structural degradation.

Structural and morphological features of fresh and recycled catalyst

To assess the structural and morphological stability of the $CuFe_2O_4$ catalyst over multiple reaction cycles, SEM and PXRD analyses were performed on both the fresh and recovered samples after five cycles of reuse (Fig. 5).

SEM images (Fig. 5a and b) of both the fresh and recycled $CuFe_2O_4$ catalyst show the presence of nanosized spherical domains distributed across the surface of larger particulate structures. The larger underlying features likely reflect agglomerated or sintered $CuFe_2O_4$ material formed during synthesis or subsequent thermal treatments.

Importantly, EDX analysis (Fig. 5c–f) confirms homogeneous elemental distribution (Cu, Fe, O) across both small and large domains, suggesting the absence of any extraneous support or carrier material. This indicates that both morphological features belong to the same $CuFe_2O_4$ phase, differing only in the degree of aggregation or surface roughness. The preservation of spherical domains and consistent elemental composition supports the physical robustness and chemical homogeneity of the catalyst under the applied reaction conditions.

PXRD patterns (Fig. 5g–i) confirm the crystalline spinel structure of $CuFe_2O_4$ in both fresh and recycled catalysts. The fresh catalyst shows characteristic diffraction peaks at $2\theta \approx$ 18.9° (111), 30.2° (220), 35.4° (311), 37.6° (222), 43.1° (400), 53.6° (422), 57.6° (511), 62.5° (440), and 74.7° (533), in good agreement with the standard pattern for cubic $CuFe_2O_4$ (JCPDS no. 34-0425). After five catalytic cycles, all major peaks are preserved in the recycled sample, indicating that the spinel structure remains intact without phase decomposition. A slight broadening and reduction in peak intensities are observed in the recycled sample (Fig. 5h), which may result from surface-level modifications, minor agglomeration, or decreased long-range ordering associated with repeated heating and magnetic separation. In the recycled sample, two additional weak reflections appear at $2\theta \approx$ 23.10° and 27.08°, which do not correspond to $CuFe_2O_4$. These peaks likely originate from carbonaceous residues formed during reaction cycles involving organic substrates, and their presence does not impact the integrity of the ferrite phase. Upon calcination of the recycled catalyst at 400 °C for 2 h, these low-angle peaks disappear, confirming the thermal removal of residual organic deposits. However, new weak reflections emerge at $2\theta \approx$ 48.09°, 66.02°, and 68.21°, which are not present in the fresh catalyst and are attributed to minor surface oxidation or phase restructuring during calcination, possibly due to the formation of low-percentage CuO or spinel-related secondary domains. The peak at 48.09° may correspond to the (200) reflection of monoclinic CuO, while those at 66.02° and 68.21° can be linked to higher-order reflections of surface-generated copper oxide phases. These changes are limited to surface regions and do not indicate any structural decomposition of the core $CuFe_2O_4$ phase. However, these differences are minimal and do not
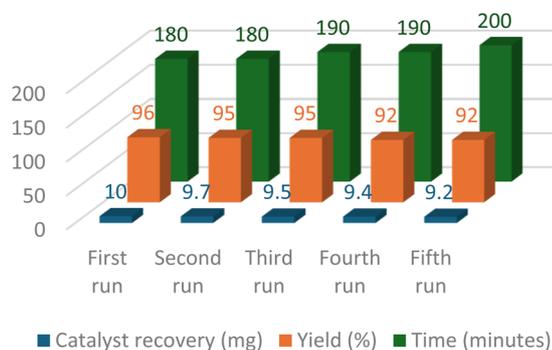

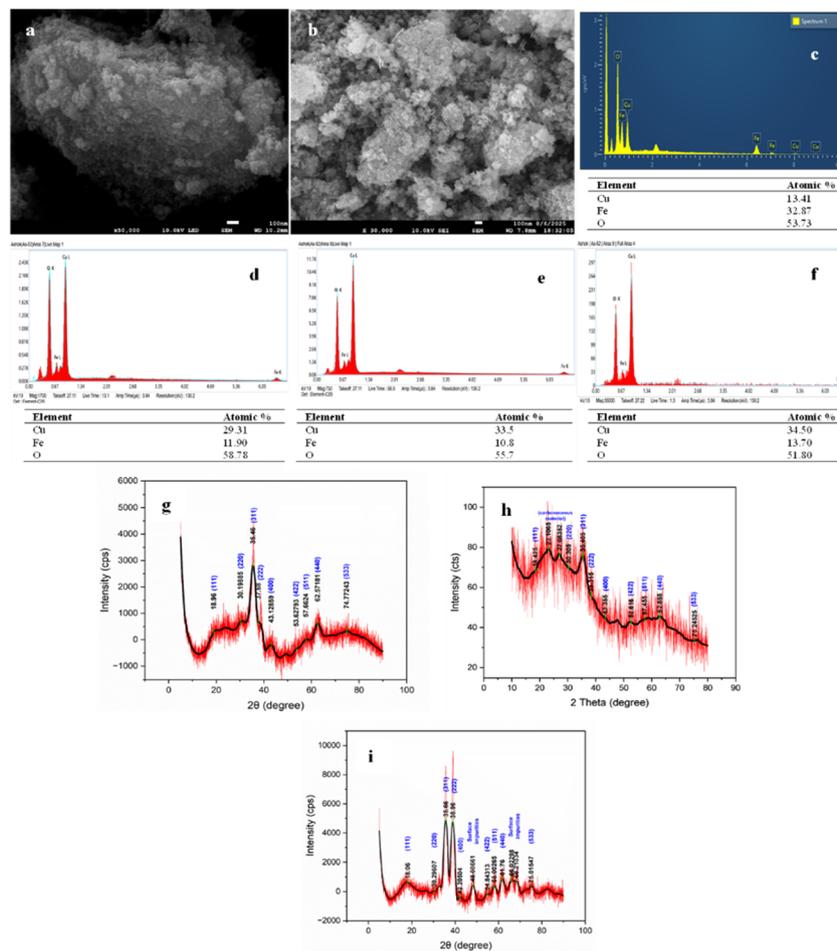**Fig. 4** Reusability and recovery of $CuFe_2O_4$ nanoparticles.

Fig. 5 (a) SEM of fresh catalyst; (b) SEM of recycled catalyst; (c) EDX of small spherical domain (fresh); (d) EDX of large domain (fresh); (e) EDX of small spherical domain (recycled); (f) EDX of large domain (recycled); (g) PXRD of fresh catalyst; (h) PXRD of recycled catalyst after 5 cycles without calcination; (i) PXRD of recycled catalyst after calcination at 400 °C for 2 h.

imply any significant compromise in crystallinity or performance.

The crystallite size of the fresh and recycled catalyst was calculated using the Debye–Scherrer equation:

$$D = (k \times \lambda)/(\beta \cos \theta)$$

where D is the crystallite size, k is a shape factor (0.94), λ is the X-ray wavelength (1.5406 Å), and β is the broadening of the diffraction line measured at half maximum intensity in radians, calculated as follows:

$$\beta = \text{FWHM (°)} \times \pi/180$$

and θ is the Bragg's angle. The (311) and (440) reflections at $2\theta \approx 35.46°$ and $62.57°$ for the fresh catalyst yielded crystallite sizes of 4.34 nm and 4.90 nm, respectively. The average crystallite size was thus calculated to be 4.62 ± 0.28 nm, supporting the nanocrystalline nature of the material.

For the recycled catalyst, the corresponding reflections appeared at $2\theta \approx 35.66°$ and $61.76°$, giving crystallite sizes of 10.59 nm and 9.25 nm, respectively, with an average value of 9.92 ± 0.67 nm. The increase in crystallite size after calcination and reuse suggests partial growth or sintering of crystallites during thermal and catalytic cycling. The crystallite size data for both samples is presented in Table 2.

Table 2 Crystallite size estimation of fresh and recycled $CuFe_2O_4$ using the Debye–Scherrer equation

Diffraction plane	2θ (°)		θ (°)		FWHM (radians)		Crystallite size (nm)	
	Fresh	Recycled	Fresh	Recycled	Fresh	Recycled	Fresh	Recycled
(311)	35.46	35.66	17.73429	17.83	0.03501	0.01436	4.34	10.59
(440)	62.57	61.76	31.28565	30.88	0.03461	0.01825	4.90	9.25
Average							4.62 ± 0.28	9.92 ± 0.67

Together, the SEM and PXRD analyses demonstrate that $CuFe_2O_4$ retains its structural integrity and morphology after prolonged use, reinforcing its suitability as a robust and recyclable heterogeneous catalyst for this transformation.

Conclusions

In summary, we have developed an efficient one-pot protocol for the synthesis of α-aryl-2-benzofuranmethamines *via* a $CuFe_2O_4$-catalyzed tandem A^3 coupling, 5-*exo*-dig cyclization, and 1,3-allylic rearrangement sequence. The method proceeds under mild conditions using a magnetically recoverable, economical $CuFe_2O_4$ catalyst with excellent reusability, in the presence of Cs_2CO_3 as base and 1,4-dioxane as solvent. The transformation accommodates a good substrate scope and consistently delivers good to excellent yields (80–96%) in shorter reaction times with operational simplicity. Mechanistic insights suggest the involvement of Cu^{2+} and Fe^{3+} Lewis acidic sites in promoting key bond-forming steps, while the base plays a critical role in enabling both cyclization and rearrangement. The catalyst retained its activity over five cycles with minimal structural or morphological degradation. Overall, this strategy offers a sustainable and step-economical route to access medicinally relevant α-substituted 2-benzofuranmethamines, addressing key limitations associated with previously reported multistep methods.

Experimental

General information

Salicyaldehyde, 5-chlorosalicylaldehyde, phenylacetylene, 4-methylphenylacetylene, all cyclic secondary amines, caesium carbonate, copper chloride ($CuCl_2 \cdot 2H_2O$), and ferrous chloride ($FeCl_2 \cdot 4H_2O$) were procured from commercial suppliers and used without further purification. The progress of the reaction was monitored by Thin Layer Chromatography (TLC) on Merck-made silica gel 60-F-254 aluminium plates. The melting points were determined in open capillary tubes and were uncorrected. XPS analysis was conducted on a Thermo Scientific NEXA Surface Analyzer, and XRD patterns were obtained with a PAN-alytical EMPYREAN model. Nova nano FE-SEM 450 (FEI) was used to record SEM-EDX. NMR spectra, including both ^{1}H NMR and ^{13}C NMR, were recorded on a Jeol/ECZ 500R/S1 spectrometer operating at 500 MHz, with $CDCl_3$ as the solvent, and chemical shifts were reported in ppm. Mass spectra were recorded on a Xevo G2-S Q Tof (Waters, USA) Mass spectrometer (direct mass ESI-APCI).

Synthesis of $CuFe_2O_4$ nanoparticles

$CuFe_2O_4$ nanoparticles were synthesized *via* a soft chemical co-precipitation method, following a previously reported procedure.[15] A 50 mL aqueous solution of $CuCl_2 \cdot 2H_2O$ (0.1 mmol, 0.8524 g) was combined with a 100 mL aqueous solution of $FeCl_2 \cdot 4H_2O$ (0.1 mmol, 1.9800 g) in a 1 : 2 molar ratio under vigorous stirring at room temperature. A concentrated NaOH solution was then added dropwise until the pH reached 13. A

black precipitate of $CuFe_2O_4$ nanoparticles formed, which was collected by centrifugation at 6000 rpm for 20 minutes and subsequently decanted. The precipitate was washed repeatedly with distilled water until the washings reached neutral pH (∼7), and the material was dried to afford $CuFe_2O_4$ as a fine black powder.

General procedure for the synthesis of α-aryl-2-benzofuranmethamines (5a–h)

A mixture of substituted salicylaldehyde (1.0 mmol), cyclic secondary amine (1.2 mmol), and substituted phenylacetylene (1.3 mmol) was combined with Cs_2CO_3 (0.31 mmol, 0.10 g), and $CuFe_2O_4$ nanoparticles (10 mg, 4.4 mol%) in 1,4-dioxane (5.0 mL) in a round-bottom flask. The reaction mixture was stirred at 80 °C for 3 hours. The progress of the reaction was monitored by TLC using ethyl acetate/hexane (2 : 8) as the mobile phase. Upon completion, the catalyst was separated using an external magnet, washed thoroughly with petroleum ether, and dried at 60 °C for 3 hours for reuse.

The reaction mixture was then concentrated under reduced pressure, and the crude residue was purified by column chromatography using ethyl acetate/hexane (1 : 9) as the eluent to afford the corresponding α-aryl-2-benzofuranmethamine derivatives (5a–h) as pure products.

1-(Benzofuran-2-yl(phenyl)methyl)piperidine (5a)

The title compound was prepared following the general procedure comprising salicylaldehyde (1.0 mmol, 0.12 mL), phenyl-acetylene (1.1 mmol, 0.14 mL), 3-methylpiperidine (1.3 mmol, 0.145 mL), cesium carbonate (0.31 mmol, 0.10 g), and $CuFe_2O_4$ (4.4%, 10 mg) in 5 mL of dioxane providing a yellow colored solid. Yield: 0.290 g, 96%; R_f = 0.21 (ethylacetate/hexane 1 : 9); mp: 96–97 °C; ^{1}H-NMR (500 MHz, $CDCl_3$/TMS), δ (ppm): 7.63–7.24 (m, 9H), 6.91 (s, 1H), 4.14 (s, 1H), 3.11 (m, 3H), 2.73 (t, 1H), 1.78 (m, 5H), 0.93 (s, 3H); ^{13}C-NMR (500 MHz, $CDCl_3$), δ (ppm): 153.61, 149.16, 138.70, 132.66, 130.12, 129.35, 128.74, 128.61, 126.85, 126.19, 123.82, 121.90, 111.64, 74.07, 61.13, 32.01, 29.66, 22.85, 19.55. HRMS (ESI) *m/z*: $[M + H]^+$ calcd for $C_{21}H_{23}NO + H^+$, 306.1813; found, 306.1819.

Author contributions

Ashok Kumar Raigar carried out the investigation and played a supporting role in validation and literature survey. Manju and Kamlesh Saini contributed to supporting roles in the literature survey. Anjali Guleria conceived and supervised the project, developed the methodology, curated and validated the data, managed project administration and visualization, contributed to the literature survey, wrote the original draft, and led the final review and editing of the manuscript.

Conflicts of interest

There are no conflicts to declare.

Data availability

The data supporting this article have been included as part of the SI. Supplementary information is available. See DOI: **https://doi.org/10.1039/d5ra05808b**.

Acknowledgements

References

1 I. A. Moussa, S. D. Banister, C. Beinat, N. Giboureau, A. Reynolds and M. Kassoiu, Design, Synthesis, and Structure−Affinity Relationships of Regioisomeric N-Benzyl Alkyl Ether Piperazine Derivatives as σ-1 Receptor Ligands, *J. Med. Chem.*, 2010, **53**, 6228–6239.

2 E. Roberts, N. Plobeck and C. Wahlestedt, Compounds with analgesic effect, *US Pat.*, US6680321Bl19970703, 2004, CAN127:149159.

3 S. Younes, G. Baziard-Mouysset, G. de Saqui-Sannes, J. L. Stigliani, M. Payard, R. Bonnafous and J. Tisne-Versailles, Synthesis and pharmacological study of new calcium antagonists, analogues of cinnarizine and flunarizine, *Eur. J. Med. Chem.*, 1993, **28**, 943–948.

4 V. Pestellini, M. Ghelardoni, C. A. Maggi, G. Roncucci and A. Meli, N-[(benzofuran-2-yl)(phenyl)methyl]-alkylene diamines useful in treating arrhythmic, histaminic and tussive conditions, *US Pat.*, US4485112A19841127, 1984, CAN102:90136.

5 N. J. McLean, H. Tye and M. Whittaker, Microwave assisted Petasis boronic-Mannich reactions, *Tetrahedron Lett.*, 2004, **45**, 993–995.

6 P. Nun, J. Martinez and F. Lamaty, Microwave-assisted neat procedure for the Petasis reaction, *Synthesis*, 2010, **2010**, 2063–2068.

7 N. Wongsa, U. Sommart, T. Ritthiwigrom, A. Yazici, S. Kanokmedhakul, K. Kanokmedhakul, A. C. Willis and S. G. Pyne, Concise synthesis of α-substituted 2-benzofuranmethamines and other 2-substituted benzofurans via α-substituted 2-benzofuranmethyl carbocation intermediates, *J. Org. Chem.*, 2013, **78**(3), 1138–1148.

8 L. Y. Ukhin, L. V. Belousova, Z. I. Orlova, M. S. Korobov and G. S. Borodkin, Dehydration Rearrangements of Derivatives of Methylenedihydrobenzofuran - a New Path to Substituted Benzofurans, *Chem. Heterocycl. Compd.*, 2002, **38**, 1174–1179.

9 R.-V. Nguyen and C.-J. Li, Efficient Synthesis of Dihydrobenzofurans via a Multicomponent Coupling of Salicylaldehydes, Amines, and Alkynes, *Synlett*, 2008, **12**, 1897–1901.

10 N. Sakai, N. Uchida and T. Konakahara, Facile and efficient synthesis of polyfunctionalized benzofurans: three-component coupling reactions from an alkynylsilane, an o-hydroxybenzaldehyde derivative, and a secondary amine by a Cu(I)–Cu(II) cooperative catalytic system, *Tetrahedron Lett.*, 2008, **49**, 3437–3440.

11 H. Li, J. Liu, B. Yan and Y. Li, New domino approach for the synthesis of 2,3-disubstituted benzo[b]furans via copper-catalyzed multi-component coupling reactions followed by cyclization, *Tetrahedron Lett.*, 2009, **50**, 2353–2357.

12 X. Zhang, D. Li, X. Jia, J. Wang and X. Fan, CuI/[bmim]OAc in [bmim]PF6: a highly efficient and readily recyclable catalytic system for the synthesis of 2,3-disubstituted benzo[b]furans, *Catal. Commun.*, 2011, **12**, 839–843.

13 (a) H. Harkat, A. Blanc, J.-M. Weibel and P. Pale, Versatile and Expeditious Synthesis of Aurones via AuI-Catalyzed Cyclization, *J. Org. Chem.*, 2008, **73**, 1620–1623; (b) B. Gabriele, R. Mancuso and G. A. Salerno, Novel Synthesis of 2-Functionalized Benzofurans by Palladium-Catalyzed Cycloisomerization of 2-(1-Hydroxyprop-2-ynyl)phenols Followed by Acid-Catalyzed Allylic Isomerization or Allylic Nucleophilic Substitution, *J. Org. Chem.*, 2008, **73**, 7336–7341; (c) M. Yu, R. Skouta, L. Zhou, H.-f. Jiang, X. Yao and C.-J. Li, Water-Triggered, Counter-Anion-Controlled, and Silver−Phosphines Complex-Catalyzed Stereoselective Cascade Alkynylation/Cyclization of Terminal Alkynes with Salicylaldehydes, *J. Org. Chem.*, 2009, **74**, 3378–3383; (d) M. Yu, M. Lin, C. Han, L. Zhou, C.-J. Li and X. Yao, Ligand-promoted reaction on silver nanoparticles: phosphine-promoted, silver nanoparticle-catalyzed cyclization of 2-(1-hydroxy-3-arylprop-2-ynyl)phenols, *Tetrahedron Lett.*, 2010, **51**, 6722–6725; (e) M. Lin, M. Yu, C. Han, C.-J. Li and X. Yao, Ligand-promoted reaction on silver nanoparticles: phosphine-promoted, silver nanoparticle-catalyzed cyclization of 2-(1-hydroxy-3-arylprop-2-ynyl)phenols, *Synth. Commun.*, 2011, **41**, 3228–3236; (f) X. Li, J. Xue, R. Chen and Y. Li, A New Copper(I)-Catalyzed Cycloetherification/Acid-Catalyzed Allylic Nucleophilic Substitution for One-Pot Synthesis of 2-Substituted Benzofurans, *Synlett*, 2012, **23**, 1043–1046; (g) H. Yin, Y. Wu, X. Gu, Z. Feng, M. Wang, D. Feng, M. Wang, Z. Cheng and S. Wang, Synthesis of pyrano [3, 2-c] quinolones and furo [3, 2-c] quinolones via acid-catalyzed tandem reaction of 4-hydroxy-1-methylquinolin-2 (1 H)-one and propargylic alcohols, *RSC Adv.*, 2022, **12**(33), 21066–21078; (h) J. Zhang and Z. He, Lewis Base-Catalyzed Intramolecular Vinylogous Aldol Reaction and Chemoselective Syntheses of 3-Hydroxy-2, 3-Disubstituted Dihydrobenzofurans and Indolines, *J. Org. Chem.*, 2023, **88**(18), 13102–13114.

14 (a) R. Zhang, C. Miao, Z. Shen, S. Wang, C. Xia and W. Sun, Magnetic Nanoparticles of Ferrite Complex Oxides: A Cheap, Efficient, Recyclable Catalyst for Building the C-N Bond

under Ligand-Free Conditions, *ChemCatChem*, 2012, **4**, 824–830; (*b*) S. Ahammed, D. Kundu and B. C. Ranu, Cu-Catalyzed Fe-Driven Csp–Csp and Csp–Csp2 Cross-Coupling: An Access to 1,3-Diynes and 1,3-Enynes, *J. Org. Chem.*, 2014, **79**, 7391–7398; (*c*) G. Satish, K. H. V. Reddy, K. Ramesh, B. S. P. A. Kumar and Y. V. D. Nageswar, An elegant protocol for the synthesis of N-substituted pyrroles through C–N cross coupling/aromatization process using CuFe$_2$O$_4$ nanoparticles as catalyst under ligand-free conditions, *Tetrahedron Lett.*, 2014, **55**, 2596–2599; (*d*) A. R. Hajipour, M. Karimzadeh and G. Azizi, Highly efficient and magnetically separable nano-CuFe$_2$O$_4$ catalyzed S-arylation of thiourea by aryl/heteroaryl halides, *Chin. Chem. Lett.*, 2014, **25**, 1382–1386; (*e*) G. Satish, K. H. V. Reddy, B. S. P. Anil, K. Ramesh, R. U. Kumar and Y. V. D. Nageswar, Direct C–H arylation of benzothiazoles by magnetically separable nano copper ferrite, a recyclable catalyst, *Tetrahedron Lett.*, 2015, **56**, 4950–4953; (*f*) A. H. Elwahy and M. R. Shaaban, Synthesis of heterocycles catalyzed by iron oxide nanoparticles, *Heterocycles*, 2017, **94**(4), 595–655; (*g*) F. Nemati, M. Kaveh, A. Elhampour and M. S. Mirhosseyni, Cu$_2$O/Nano-CuFe$_2$O$_4$ as a Magnetically Recoverable Catalyst for Ligand-Free Synthesis of Imidazo [1,2-*a*] Pyridines and 3-Aroylimidazo[1,2-*a*] Pyridines, *Natl. Acad. Sci. Lett.*, 2019, **42**, 479–484; (*h*) M. Ghobadi, Based on copper ferrite nanoparticles (CuFe$_2$O$_4$ NPs): catalysis in synthesis of heterocycles, *J. Synth. Chem.*, 2022, **1**(2), 84–96; (*i*) S. Sharma, P. Jakhar and H. Sharma, CuFe$_2$O$_4$ nanomaterials: current discoveries in synthesis, catalytic efficiency in coupling reactions, and their environmental applications, *J. Chin. Chem. Soc.*, 2023, **70**(2), 107–127; (*j*) R. Veligeti, J. S. Anireddy, R. B. Madhu, A. Bendi, P. L. Praveen and D. S. Ramakrishna, Solvent-free synthesis of acridone based dihydropyrazine derivatives using CuFe2O4 nanoparticles as heterogeneous catalyst: molecular docking and in-vitro studies as anticancer agents, *J. Inorg. Organomet. Polym. Mater.*, 2023, **33**(12), 4039–4051; (*k*) D. Sanap, L. Avhad, S. Ahire, M. Mirzaei, D. Kumar, S. Ghotekar and N. D. Gaikwad, Insights into the promising heterogeneous catalysis of eco-friendly synthesized spinel CuFe2O4 nanoparticles for Biginelli reaction, *Res. Chem. Intermed.*, 2024, **50**(8), 3687–3711.

15 M. L. Kantam, J. Yadav, S. Laha and S. Jha, Synthesis of Propargylamines by Three-Component Coupling of Aldehydes, Amines and Alkynes Catalyzed by Magnetically Separable Copper Ferrite Nanoparticles, *Synlett*, 2009, **2009**, 1791–1794.